

# Mechanistic Implications of the Assembly of Organic Thiocyanates on Precious Metals

Jacob W. Ciszek and James M. Tour\*

Department of Chemistry and Center for Nanoscale Sciences and Technology, Rice University, 6100 Main Street, Houston, Texas 77005

Received May 16, 2005. Revised Manuscript Received September 13, 2005

Thiocyanate assembly is shown to be an effective method for assembling thiolate structures on platinum, silver, and gold. The assemblies were studied by infrared reflection spectroscopy and X-ray photoelectron spectroscopy (XPS). Two cyanide species were identified on the surfaces: the first corresponding to adsorbed cyanide and the second to a form commonly seen as an intermediate during cyanide etching of metals. The presence of the second species supports the theory that cyanide is leaving the surface as  $M(CN)_x$ , resulting in a thiolate monolayer. Comparison of thiocyanate assemblies on evaporated gold and silver to those on template-stripped gold demonstrates the integral role of surface morphology in the expulsion of  $(CN)_{ads}$  from the surface of the metals.

## Introduction

The assembly of organic thiocyanates has recently been demonstrated on evaporated gold surfaces.<sup>1</sup> This new process for the formation of self-assembled monolayers has the advantage that it does not require exogenous deprotection additives nor an oxygen-free system for assembly. In addition, thiocyanates are more stable than traditional thiols; this is especially important for aromatic variants where the thiol oxidative instability rapidly leads to disulfide formation and often subsequent precipitation. The thiocyanate assembly on gold also gives the same thiolate bonding structure as thiol assemblies with no sign of cyanide contamination. The hypothesized mechanism is a surface-mediated reduction of the thiocyanate, with the cyanide leaving as  $[Au(CN)_2]^-$  (Figure 1).

At the time of our report,<sup>1</sup> little evidence was available for the hypothesized mechanism. Part of the difficulty in obtaining such confirmation is the nature of the  $Au(CN)_{ads}$  species since it is rarely present in large concentrations, and isolating the trace  $[Au(CN)_2]^-$  generated by the reaction is difficult. This is further compounded by the dearth of literature concerning cyanide-related adsorbates on gold,<sup>2–5</sup> which is due in part to the propensity of such solutions to etch the surface. Therefore, for further clarification of the mechanistic aspects of thiocyanate assembly, we have performed assemblies on platinum and silver. The differences between substrates and their respective thiolate monolayers allow us to make more definitive statements about the

assembly mechanism. Silver differs from gold in many properties including work function,<sup>6</sup> surface energy,<sup>7</sup> surface energy heterogeneity,<sup>8</sup> and monolayer packing density.<sup>9</sup> For platinum, the well-characterized  $Pt(CN)_{ads}$  state gives us ample opportunity to analyze the different adsorbed states, which will allow for parallels to the  $Au(CN)_{ads}$  state. The free thiol assemblies are known for these precious metals,<sup>10–13</sup> and both silver and platinum assemblies occur in a manner similar to that of the gold–thiol assemblies with the caveat that silver and platinum are prone to surface oxidation, which interferes with the assemblies. Thus, care must be taken to exclude oxygen during the assembly processes on silver and platinum. Though this mitigates some of the advantages of the thiocyanate system, the insight garnered from these assemblies is required to gain a better understanding of the mechanism of thiocyanate assembly on gold.

## Experimental Section

**Materials.** 1-Dodecanethiol and 1-octanethiol were obtained from Aldrich. The synthesis of  $C_8H_{17}SCN$  can be found in the Supporting Information. All other compounds were prepared as described previously.<sup>1</sup> Ethanol (100%) was obtained from Pharmco. THF was freshly distilled (sodium, benzophenone) prior to use. All metals were of 99.99% or greater purity. Silicon (100) wafers (p-doped, test grade) were obtained from Silicon Quest International.

**Preparation of Evaporated Metal Substrates.** All metal substrates were prepared by e-beam evaporation with a base pressure

\* To whom correspondence should be addressed. E-mail: tour@rice.edu.

- (1) Ciszek, J. W.; Stewart, M. P.; Tour, J. M. *J. Am. Chem. Soc.* **2004**, *126*, 13172–13173.
- (2) Han, P.; Sykes, E. C. H.; Pearl, T. P.; Weiss, P. S. *J. Phys. Chem. A* **2003**, *107*, 8124–8129.
- (3) Yamada, T.; Sekine, R.; Sawaguchi, T. *J. Chem. Phys.* **2000**, *113*, 1217–1227.
- (4) Gao, P.; Weaver, M. J. *J. Phys. Chem.* **1989**, *93*, 6205–6211.
- (5) Kunitatsu, K.; Seki, H.; Golden, W. G.; Gordon, J. G. I.; Philpott, M. R. *Langmuir* **1988**, *4*, 337–341.

- (6) Dhirani, A.; Hines, M. A.; Fisher, A. J.; Ismail, O.; Guyot-Sionnest, P. *Langmuir* **1995**, *11*, 2609–2614.
- (7) Skriver, H. L.; Rosengard, N. M. *Phys. Rev. B* **1992**, *46*, 7157–7168.
- (8) Sellers, H.; Ulman, A.; Shnidman, Y.; Eilers, J. E. *J. Am. Chem. Soc.* **1993**, *115*, 9389–9401.
- (9) Fenter, P.; Eisenberger, P. *Langmuir* **1991**, *7*, 2013–2016.
- (10) Li, Z.; Chang, S.-C.; Williams, R. S. *Langmuir* **2003**, *19*, 6744–6749.
- (11) Walczak, M. M.; Chung, C.; Stole, S. M.; Widrig, C. A.; Porter, M. D. *J. Am. Chem. Soc.* **1991**, *113*, 2370–2378.
- (12) Hatchett, D. W.; Uibel, R. H.; Stevenson, K. J.; Harris, J. M.; White, H. S. *J. Am. Chem. Soc.* **1998**, *120*, 1062–1069.
- (13) Laibinis, P. E.; Whitesides, G. M.; Allara, D. L.; Tao, Y.-T.; Parikh, A. N.; Nuzzo, R. G. *J. Am. Chem. Soc.* **1991**, *113*, 7152–7167.

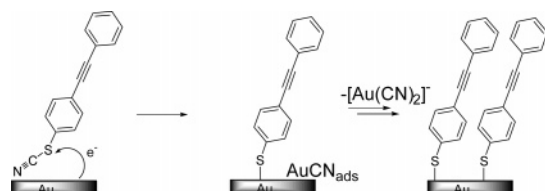


Figure 1. Initial proposed mechanism for thiocyanate assembly.

Table 1. Compounds Used for Assembly on Precious Metal Surfaces

Number	Structure
1	
2	
3	
4	

of  $\sim 1 \times 10^{-7}$  Torr on test grade  $\langle 100 \rangle$  silicon wafers with a typical evaporation rate of 2 Å/s. A titanium adhesion layer (2 nm) was applied to all substrates prior to deposition of 100 nm of the metal. All substrates were used within 20 min after removal from the vacuum chamber.

**Preparation of Template-Stripped Gold.** Template-stripped gold substrates were prepared as described previously.<sup>14,15</sup> A bare silicon substrate ( $\langle 100 \rangle$ , p-doped, test grade) was treated with Piranha solution for 10 min. Gold was thermally evaporated at a base pressure of  $1 \times 10^{-6}$ . The initial evaporation rate was at 0.5 Å/s for the first 15 nm and then increased to 1.5 Å/s until a final thickness of between 100 and 150 nm was reached. The samples were cooled, removed from the chamber, and attached to glass slides with EPO-TEK 377. Gold substrates were removed from their silicon backing as needed.

**Assembly Preparation.** Assemblies were performed with 1 mM solutions on freshly prepared substrates and an assembly time of 20–48 h. After assembly the samples were rinsed with the same solvent used for assembly, optionally sonicated in the case of the aromatic species, and dried under a stream of nitrogen. Platinum and silver assemblies were prepared in the drybox within 5 min after their removal from the evaporation chamber. As a control, gold samples were also assembled under drybox conditions. The compounds used for assembly are listed in Table 1.

**Water Contact Angle Measurements.** Contact angle measurements were performed using a Ramé-Hart goniometer model 100. Measurements were taken on at least two locations with at least five advancements of the drop of deionized water. Values shown are the average of at least two samples.

**Ellipsometric Measurements.** Measurements of surface optical constants and molecular layer thicknesses were taken with a single wavelength (632.8 nm laser) LSE Stokes Ellipsometer (Gaertner Scientific). The surface thickness was modeled as a single absorbing layer atop an infinitely thick substrate (fixed  $n_s$ ). The observed error in repeated measurements of the same spot was typically 0.2 nm or less. The index of refraction was set at 1.45 for aliphatic assemblies and 1.55 for aromatic compounds.

**Infrared Reflection Spectroscopy Measurements.** A Nicolet Nexus 670 spectrometer with KBr beam splitter and MCT/A

detector was used in conjunction with a SMART/SAGA grazing angle accessory, using a 16 mm diameter sampling area with p-polarized light fixed at an 80° angle of incidence.

**X-ray Photoelectron Spectroscopy (XPS) Measurements.** A PHI Quantera SXM XPS/ESCA system at  $5 \times 10^{-9}$  Torr was used to take photoelectron spectra. A monochromatic Al X-ray source at 100 W was used with an analytical spot size of 0.15 mm  $\times$  1.4 mm and a 45° takeoff angle, with pass energy of 26.00 eV. High-resolution spectra of the S 2p region used a 45° takeoff angle and 13.00 eV pass energy. Unless noted, surface samples were referenced against internal Au 4f<sub>7/2</sub> line at 84.0 eV, Ag 3d<sub>5/2</sub> at 368.3 eV, or Pt 4f<sub>7/2</sub> 71.2. Powder XPS photoelectron lines were referenced against the C 1s signal at 284.50 eV.

## Results

**Thiocyanates on Gold.** Of all the metals, gold is the only substrate where thiocyanate assembly has been demonstrated.<sup>1</sup> It is known that thiocyanates react with gold to give the same thiolate bound monolayer as produced when starting with the free thiol. In the initial communication it was reported that the transient species (CN)<sub>ads</sub> was observed in a few cases. This observation warrants further analysis.

The analysis of a large number of assemblies shows a number of samples that contain no surface nitrogen (as seen by the N 1s signal in XPS) as well as a number of incomplete assemblies that do contain some nitrogen signal. The upper limit of assembly quality can be seen in Figures 2a and 2b where the signal-to-noise (acquired over 12 h) shows that if any nitrogen signal is present, it is less than 5% relative to the sulfur signal. For all cases where nitrogen was seen, the relative atomic concentration of nitrogen versus sulfur on the surface can be used as a rough indication of the number of surface sites (( $\sqrt{3} \times \sqrt{3}$ )R30° for aliphatics, ( $2\sqrt{3} \times \sqrt{3}$ )-R30° for aromatics, Figures 3a–3f)<sup>16,17</sup> occupied by those two elements. Contact angle and ellipsometry clearly support this assumption for the aliphatic species. Experiments with mixed disulfide monolayers (R–S–S–R', where R and R' are shown to be present on the surface in equal amounts but where R' has minimal height) show that ellipsometry, and to a lesser extent contact angles, can be used as a rough indication of coverage by the longer species.<sup>18</sup>

Comparison of the these ellipsometric and contact values for organic thiocyanates to thiol controls show a difference in properties commensurate for a monolayer where a certain portion of the ( $\sqrt{3} \times \sqrt{3}$ ) sites (roughly equal to the N to S ratio) have been occupied by Au(CN)<sub>ads</sub> in the thiocyanate assemblies. This is shown in Table 2 where both the thickness and contact angles are significantly lower than those of their thiol counterparts. In the case of the aromatic species the contact angle and ellipsometry measurements for the thiol and thiocyanates are nearly identical, suggesting that if CN is adsorbed on the surface, the majority of this species is incorporated into other sites on the surface rather than replacing sulfur in the ( $2\sqrt{3} \times \sqrt{3}$ )R30° lattice. Cyclic voltammetry studies<sup>1</sup> of the monolayers support this finding, though this cannot be used quantitatively.

(14) Stamou, D.; Gourdon, D.; Leley, M.; Burnham, N. A.; Kulik, A.; Vogel, H.; Duschl, C. *Langmuir* **1997**, *13*, 2425–2428.

(15) Blackstock, J. J.; Li, Z.; Freeman, M. R.; Stewart, D. R. *Surf. Sci.* **2003**, *546*, 87–96.

(16) Ulman, A. *Chem. Rev.* **1996**, *96*, 1533–1554.

(17) Dhirani, A.-A.; Zehner, R. W.; Hsung, R. P.; Guyot-Sionnest, P.; Sita, L. R. *J. Am. Chem. Soc.* **1996**, *118*, 3319–3320.

(18) Biebuyck, H. A.; Whitesides, G. M. *Langmuir* **1993**, *9*, 1766–1770.

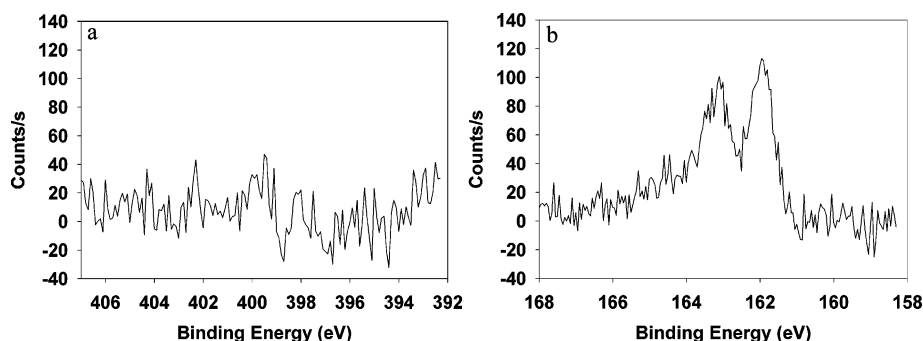


**Figure 2.** (a) Lack of a signal in the N 1s XPS region of assembled **1** on gold. (b) S 2p XPS region of assembled **1** on gold.

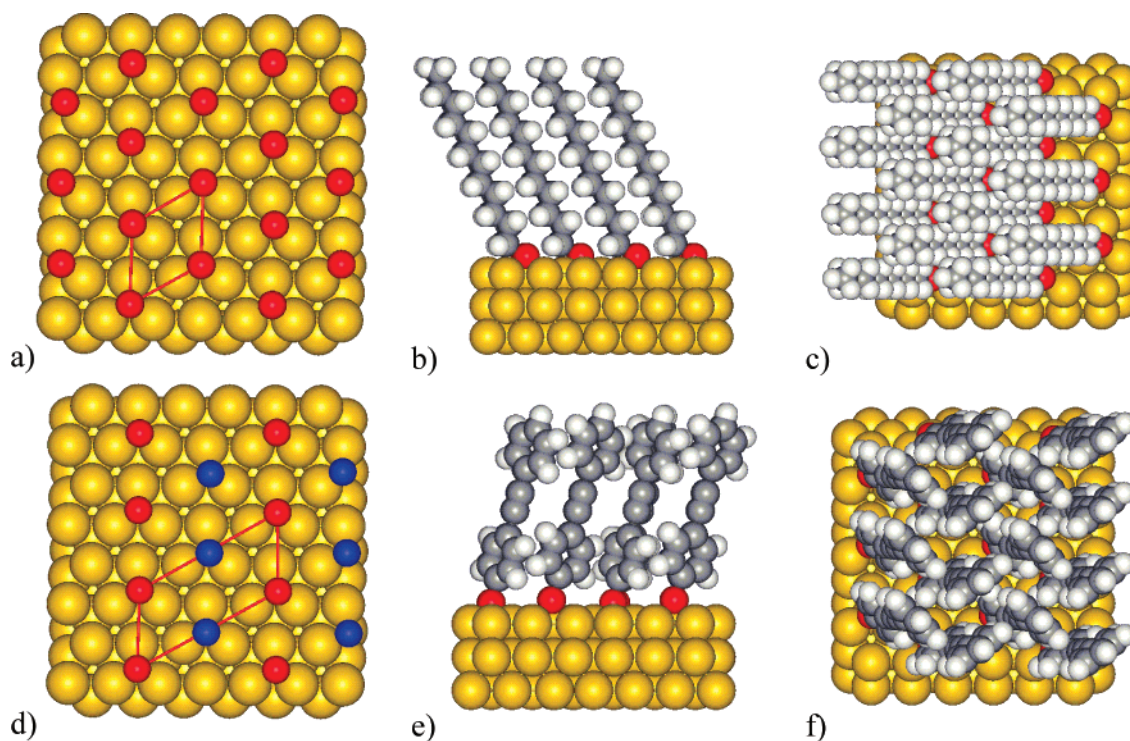


**Figure 3.** Packing structures of thiols on gold (111). (a)  $(\sqrt{3} \times \sqrt{3})R30^\circ$  sulfur structure on a gold (111) surface. (b) The same lattice with a dodecanethiolate species. (c) A top view of (b). (d)  $(2\sqrt{3} \times \sqrt{3})R30^\circ$  sulfur structure for aromatic assemblies. The blue spots represent aromatic species that are rotated  $90^\circ$  with respect to the red species in the herringbone structure.<sup>17</sup> (e) The same lattice with a short conjugated ring system. (f) A top view of (e).

**Table 2. Film Thickness ( $\pm 10\%$ ) Determined by Single Wavelength Ellipsometry and Contact Angle ( $\pm 5\%$ ) (Water) Measurements**

Molecule	Measured ellipsometric thickness ( $\text{\AA}$ )		Contact angle ( $^\circ$ , static)	
	X=SH	X=SCN	X=SH	X=SCN
$n\text{C}_{12}\text{H}_{25}\text{-X}$	16.4	12.2	105	97
	14.6	13.8	80	78

The residual  $\text{Au}(\text{CN})_{\text{ads}}$  is seen both by infrared spectroscopy and by XPS. An infrared signal is seen at  $2160\text{ cm}^{-1}$  (Figure 4a). A corresponding XPS signal is seen at 399.5 eV (Figure 4b). A second XPS N 1s peak is seen with smaller frequency and intensity and occurs at 397.9 eV (Figure 4c). A corresponding infrared frequency has not been established. Further explanation on the nature of these species can be found in the Discussion section. These signals can be seen in both the aliphatic and aromatic thiocyanate assemblies.

Some  $(\text{CN})_{\text{ads}}$  is detectable in the majority of the assemblies (for both aromatic and aliphatic thiocyanates). On evaporated gold the average over 12 identically prepared samples was 21% nitrogen on the surface (Figure 5) with a maximum of 37% and a minimum (2 samples) of no detected signal. This nitrogen signal was not seen in any of the thiol controls run side by side with thiocyanate assemblies.

The variance in nitrogen content between samples prepared from the same substrate is minimal ( $\pm 3\%$ ), but samples from different gold substrates showed a large deviation. Side by side comparisons of samples prepared with varied assembly time, thiocyanate concentration, substrate size, and chain length all show no variance in the relative concentration of nitrogen on the surface, suggesting that it is the variation of the surface morphology between substrates that determines the amount of nitrogen on the surface, and not other experimental conditions.

The assemblies were examined on template-stripped (TS) gold in order to reduce the amount of variance in the substrate between experiments. TS gold gives an extremely flat surface



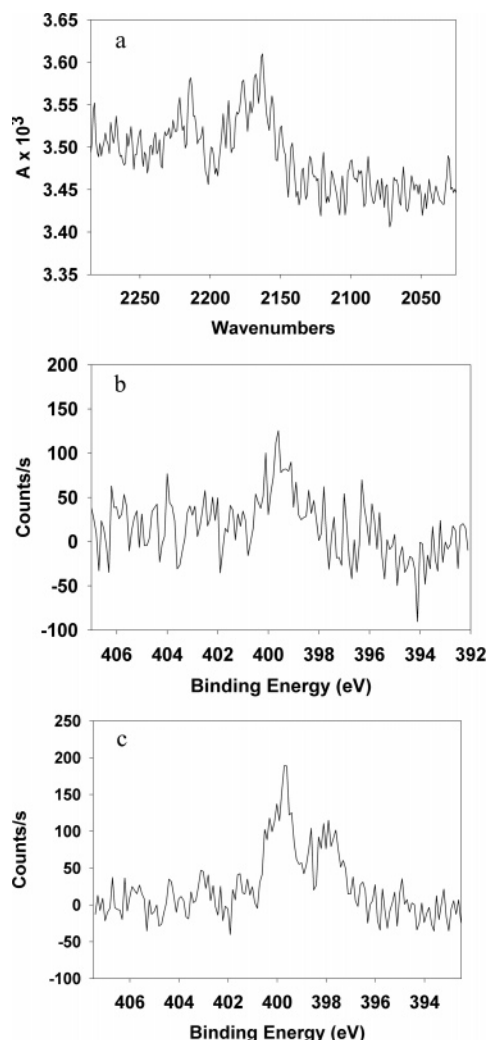


**Figure 4.** (a) Infrared reflection spectrum of assembled **2** on gold. Peak is located at  $2160\text{ cm}^{-1}$ . (b) N 1s XPS region of assembled **3** on gold. (c) N 1s XPS region of assembled **2** on gold.

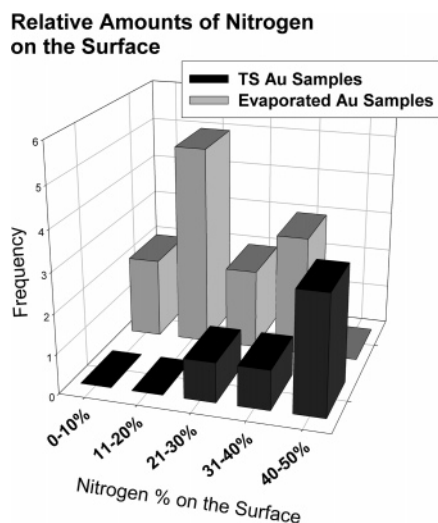


**Figure 5.** Occurrences of amounts of residual nitrogen for assemblies by XPS. Typical measurement errors are  $\pm 3\%$ . TS = template stripped.

and allows for practically unlimited storage time since the surface is protected from atmospheric contaminants and roughening.<sup>14,15</sup> With this system tens of “identical” substrates can be produced and used over a period of weeks.

The TS gold showed substantially higher residual nitrogen (39% nitrogen average) compared to the evaporated gold. It also showed a smaller standard deviation (7% nitrogen vs 11% for the evaporated gold). We attribute the higher nitrogen count to the morphology of the surface much in the way edges and defect sites play a decisive role in thiolate assemblies.<sup>19</sup> This also supports our previous assertion regarding the dependence of the concentration of surface nitrogen on substrate surface morphology since the surface morphology of evaporated gold is expected to vary from evaporation to evaporation.

**Thiocyanates on Silver.** Thiolate assemblies on silver share surprisingly few features with their gold counterparts though both pristine surfaces have similarities. For example, both the Au(111) and Ag(111) have nearly identical nearest-neighbor distances ( $2.88$  and  $2.89\text{ \AA}$ , respectively)<sup>16</sup> and are readily etched by cyanide solutions.<sup>20,21</sup> However, the thiolate monolayers have drastically different properties. Thiocyanates on silver have free energies of adsorption 45% more favorable than their counterparts on gold (1,2-benzene-dithiol).<sup>22</sup> This stability is increased in the case of aliphatic chains by the greater packing density<sup>6,9</sup> and thus larger van der Waals forces. There is also a smaller variation in energy in the surface.<sup>8</sup> As a result of this packing arrangement, Ag-(111) monolayers adopt a much smaller tilt angle ( $13^\circ$  for Ag(111) vs  $26^\circ$  for Au(111)).<sup>11,13,23</sup> The stronger chemisorption can also be seen in competitive displacement or desorption of the thiocyanates, where the rate constant on silver is an order of magnitude smaller than that of gold.<sup>24</sup> In Au-(111), the energy difference between peak and valley is  $6.0\text{ kcal/mol}$  vs  $3.3\text{ kcal/mol}$  for Ag(111).<sup>8</sup> Last, silver has a lower ionization energy ( $1.7\text{ eV}$  lower) and work function ( $0.6\text{ eV}$ )<sup>6</sup> and the metal–metal bond strength is weaker than that in gold.

Due to the much stronger lattice energy and higher packing density, we assumed that the  $\text{Ag}(\text{CN})_{\text{ads}}$  signal would be present in all samples. However, just as in the case of gold, no samples containing significant amount of  $\text{Ag}(\text{CN})_{\text{ads}}$  were found (Figure 6a). As in the case of the gold sample, the sulfur 2p signal for the thiocyanates on silver ( $161.7, 162.9\text{ eV}$ ) can be overlaid with that of free thiol assembly on the same substrate ( $161.8, 163.0\text{ eV}$ ) (Figure 6b). If the expulsion of the  $\text{M}(\text{CN})_{\text{ads}}$  adsorbate was not dominated by the surface morphology, we would expect to see a larger and more frequent appearance of  $\text{Ag}(\text{CN})_{\text{ads}}$  on the surface due to the increased intermolecular interaction of the monolayer. In some cases a  $(\text{CN})_{\text{ads}}$  XPS signal was seen at  $399.4\text{ eV}$  (N 1s).

**Thiocyanates on Platinum.** Platinum provides another comparative substrate for the thiocyanate assembly. As

- (19) Hostettler, M. J.; Templeton, A. C.; Murray, R. W. *Langmuir* **1999**, *15*, 3782–3789.
- (20) Ammen, C. W. *Recovery and Refining of Precious Metals*; Chapman & Hall: New York, 1984.
- (21) Gilchrist, J. D. *Extraction Metallurgy*, 3rd ed.; Pergamon Press: New York, 1989.
- (22) Lee, Y. J.; Jeon, I. C.; Paik, W.; Kim, K. *Langmuir* **1996**, *12*, 5830–5837.
- (23) Nuzzo, R. G.; Korenic, E. M.; Dubois, L. H. *J. Chem. Phys.* **1990**, *93*, 767–773.
- (24) Schlenoff, J. B.; Li, M.; Ly, H. *J. Am. Chem. Soc.* **1995**, *117*, 12528–12536.

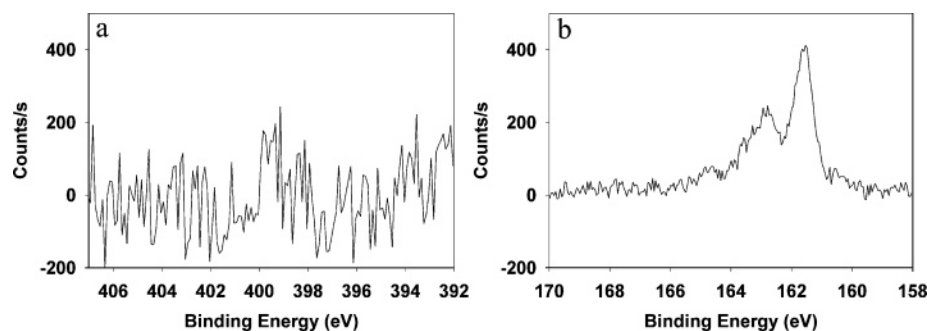


**Figure 6.** (a) Lack of signal in the N 1s XPS region of assembled **1** on silver. The spectrum has been referenced to the C 1s signal at 284.5 eV. (b) S 2p XPS region of assembled **1** on silver. The spectrum has been referenced to the C 1s signal at 284.5 eV.

opposed to gold and silver, which are easily etched by cyanide, platinum is robust to such treatment.<sup>20</sup> Since the initially proposed mechanism invokes the loss of  $[\text{Au}(\text{CN})_2]^-$  (for gold assemblies), examination of platinum assemblies may provide further evidence for or against this mechanism. Furthermore, platinum is an excellent reference since the adsorption of cyanide and cyanogen ( $(\text{CN})_2$ ) on platinum has been studied extensively<sup>25–41</sup> due to the role of  $(\text{CN})_{\text{ads}}$  in the Andrussow synthesis of HCN.<sup>42</sup>

As seen on other metals, the thiocyanate assemblies on platinum gave sulfur 2p signals (162.1, 163.3 eV) that are similar to their thiol counterparts (162.2, 163.4 eV) (Figure 7), indicating a carbon–sulfur bond cleavage and a thiolate bonding mechanism. The same residual nitrogen is seen in the platinum assemblies at 399.5 eV. It is also somewhat surprising that the ratio of sulfur to nitrogen on the surface is not 1:1; values as high as 4:1 are seen (Figure 8). The implications of this will be discussed in more detail below.

## Discussion

**Nature of the N 1s Species.** By XPS analysis, two types of residual nitrogen are seen in thiocyanate assemblies on all metals. Assignment of the peak at 397.7 eV on platinum

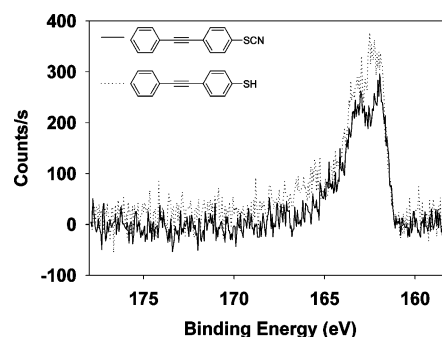


**Figure 7.** S 2p XPS region of assemblies on platinum.

(397.9 eV on gold) is made by comparing it to the well-studied adsorption of cyanide and cyanogen on platinum.<sup>25–41</sup> In the case of cyanogen adsorption on platinum, three distinct entities are seen. The first is a nondissociative adsorption of cyanogen ( $\alpha$ ), the second is dissociated “island” CN ( $\beta_1$ ), and the third is “isolated” dissociated CN ( $\beta_2$ ).<sup>28</sup> The “island” vs “isolated” cyanide shows a large difference in reactivity.<sup>26</sup> The common adsorbed states  $\alpha$ ,  $\beta_1$ , and  $\beta_2$  have their respective binding energies at 397.7, 398.0, and 397.0 eV. Adsorptions studies of HCN on platinum support these previous studies with  $(\text{CN})_{\text{ads}}$  signal assigned to the 396.9 eV<sup>25</sup> and 397.0 eV.<sup>32</sup> Levoguer and Mills<sup>32</sup> also correlate their signal with an infrared frequency of 2078  $\text{cm}^{-1}$  for  $(\text{CN})_{\text{ads}}$  parallel to the surface normal. Similar frequencies are seen for the dissociative adsorption of  $\text{CH}_3\text{CN}$ .<sup>33,34</sup> These data are consistent with studies of  $\text{CN}^-$  adsorption onto platinum electrodes which result in the same  $(\text{CN})_{\text{ads}}$  state.<sup>30,31,35</sup> The stable configuration for this is “on-top” binding with the cyanide oriented parallel to the surface normal.<sup>27,36</sup>

All of these comparisons indicate that the  $\text{M}(\text{CN})_{\text{ads}}$  we observe at 397.9/397.7 eV is clearly not on-top bonded CN ( $\beta_2$ ). A more reasonable assignment is to a state similar to the  $\beta_1$  state (island CN). The electron density on nitrogen (as seen by binding energy) is lower than that seen in the on-top binding, indicating a more electron-poor nitrogen species. To reach this lower density, the  $(\text{CN})_{\text{ads}}$  must have a higher amount of  $\pi$ -back-bonding to the metal atom.<sup>36,37</sup> This results in a weakened CN bond, which is often seen when the moiety occupies a hollow site or bridging configuration. However, we cannot rule out that the constrained environment of the monolayer is forcing the cyanide into an atypical bonding mechanism. From the data, it is clear that whatever the configuration is, this species can be identified as cyanide bound to the metal surface.

- (25) Lindquist, J. M.; Ziegler, J. P.; Hemminger, J. C. *Surf. Sci.* **1989**, *210*, 27–45.
- (26) Mills, P.; Jentz, D.; Trenary, M. J. *Am. Chem. Soc.* **1997**, *119*, 9002–9009.
- (27) Ample, F.; Clotet, A.; Ricart, J. M. *Surf. Sci.* **2004**, *558*, 111–121.
- (28) Hoffmann, W.; Bertel, E.; Netzer, F. P. *J. Catal.* **1979**, *60*, 316–324.
- (29) Ashley, K.; Lazaga, M.; Samant, M. G.; Seki, H.; Philpott, M. R. *Surf. Sci.* **1989**, *219*, L590–L594.
- (30) Stuhlmann, C. *Surf. Sci.* **1995**, *335*, 221–226.
- (31) Kim, C. S.; Korzeniewski, C. *J. Phys. Chem.* **1993**, *97*, 9784–9787.
- (32) Levoguer, C. V.; Nix, R. M. *J. Chem. Soc., Faraday Trans.* **1996**, *92*, 4799–4807.
- (33) Dederichs, F.; Petukhova, A.; Daum, A. *J. Phys. Chem. B* **2001**, *105*, 5210–5216.
- (34) Sexton, B.; Hughes, F. *Surf. Sci.* **1984**, *140*, 227–248.
- (35) Stuhlmann, C.; Villegas, I.; Weaver, M. J. *Chem. Phys. Lett* **1994**, *219*, 319–324.
- (36) Daum, W.; Dederichs, F.; Muller, J. E. *Phys. Rev. Lett.* **1998**, *80*, 766–769.
- (37) Anderson, A. B.; Kotz, R.; Yeager, E. *Chem. Phys. Lett* **1981**, *82*, 130–134.
- (38) Volmer, M.; Stratmann, M.; Viehhaus, H. *Surf. Interface Anal.* **1990**, *16*, 278–282.
- (39) Kubas, G. J.; Jones, L. H. *Inorg. Chem.* **1974**, *13*, 2816–2819.
- (40) Yau, J.; Mingos, M. P. *J. Chem. Soc., Dalton Trans.* **1997**, 1103–1111.
- (41) Daum, W.; Friedrich, K. A.; Klunker, C.; Knabben, D.; Stimming, U.; Ibach, H. *Appl. Phys. A* **1994**, *59*, 553–562.
- (42) Satterfield, C. N. *Heterogeneous Catalysis in Practice*; McGraw-Hill: New York, 1980.

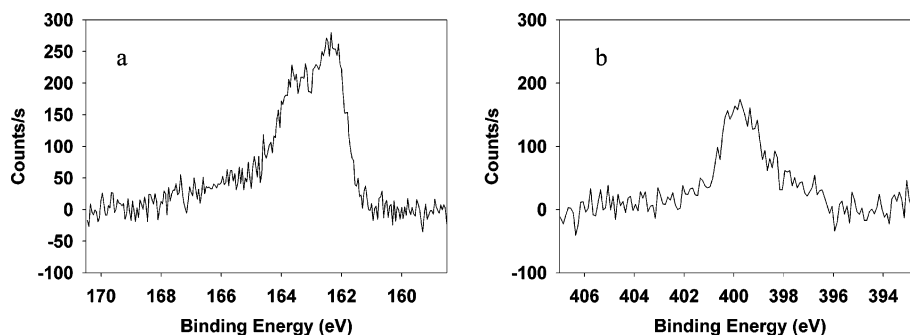


Figure 8. (a) S 2p XPS region of assembled **1** on platinum. (b) N 1s XPS region of assembled **1** on platinum.

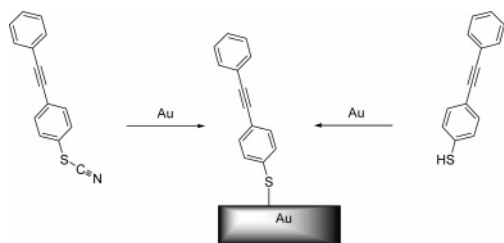


Figure 9. Thiols and thiocyanates give the same thiolate-bonded molecule on the surface.



Figure 10. Electrochemical reactions responsible for the etching of platinum and gold by cyanide.

The  $(\text{CN})_{\text{ads}}$  on the surface is clearly independent of the thiol moiety as observed by a change in the binding energy of the sulfur of the thiocyanate. Aromatic thiocyanates typically have a binding energy of 164.8 and 166.0 eV corresponding to the S 2p<sup>3/2</sup> and S 2p<sup>1/2</sup> signals. Assemblies of these species show a dramatic shift in the binding energy corresponding to a large increase of electron density on the sulfur (162.0 and 163.3 eV).<sup>1</sup> This binding energy is identical to that seen in analogous free thiol assemblies and indicates that the sulfur ends up in the same thiolate species as when starting with the free thiol (Figure 9).<sup>1</sup> The presence of  $\text{CN}_{\text{ads}}$  indicates that this is a surface-mediated reaction rather than a solution phase decomposition of the thiocyanate.

The second nitrogen species is distinguished by the infrared peak at 2160 cm<sup>-1</sup> and the XPS signal at 399.5 eV and has implications on the mechanism of  $(\text{CN})_{\text{ads}}$  displacement off the surface. This species has a stretching frequency substantially higher than any of the  $(\text{CN})_{\text{ads}}$  species on gold<sup>4,5</sup> or platinum<sup>30,31,33,35</sup> and is even higher than the frequency of  $[\text{Au}(\text{CN})_2]^-$  or  $[\text{Pt}(\text{CN})_4]^{2-}$ .<sup>39,40</sup> This species is well-known for platinum<sup>31,35,41,43</sup> (as well as palladium<sup>29</sup>) and does not come from  $(\text{CN})_{\text{ads}}$  but rather from the intermediate in the formation of  $[\text{Pt}(\text{CN})_4]^{2-}$ . It was reported previously that infrared adsorption of this intermediate appears at 2160 cm<sup>-1</sup> at 0.1 V<sup>33</sup> (moving to lower wavenumbers at higher potentials) and is tentatively assigned to  $[\text{Pt}(\text{CN})_2]^{2-}$ .<sup>31,43</sup> Au-(CN) adsorbed on the gold surface shares a similar frequency (2160 cm<sup>-1</sup>) with its platinum counterparts, suggesting that this is the nature of our second cyanide species on gold.<sup>3</sup> XPS lends further support to this assignment. As mentioned

earlier, the electron density (as seen by the N 1s binding energy) is too high (399.5 eV) for CN adsorbed onto the surface. The binding energy is very close to the species at 399.3 eV as seen for  $\text{K}_2\text{Pt}(\text{CN})_4$ <sup>44</sup> and indicates that the cyanide state is much closer to the leached metal species than the linearly adsorbed state. The possibility that molecules bonded to the surface through the nitrogen lone pair could give this same XPS signal<sup>34,45</sup> can be discounted due to the lack of a R-S-CN sulfur signal in the XPS spectra (see Supporting Information). We have observed this signal and the signal at 397.7 eV when pristine gold is exposed to a solution of  $\text{KCN}_{\text{aq}}$  and then thoroughly rinsed. When KCN was added to the thiocyanate solutions the expulsion of residual  $(\text{CN})_{\text{ads}}$  was not enhanced, but the KCN did cause slow etching of the surface to occur, presumably through defect sites in the monolayer.

The spectroscopic evidence supports a mechanism for  $(\text{CN})_{\text{ads}}$  expulsion from the surface as  $\text{M}(\text{CN})_x$ . Other mechanisms for the expulsion of  $(\text{CN})_{\text{ads}}$  as CN is unlikely since CN is an unstable radical species. The relative bond strengths of Au-S, Au-Au, and Au-CN are approximately 40, 53, and 90 kcal/mol, respectively,<sup>16,46,47</sup> also making expulsion of CN unfavorable. The same bond strength argument applies to expulsion of  $\text{CN}^-$ . The only other option, without  $\text{M}(\text{CN})_x$  loss, is the expulsion of cyanogen. Temperature-programmed desorption (TPD) experiments, however, show that a temperature of ~370 K is required to desorb molecular cyanogen and ~750 K is required for the removal of dissociated cyanogen off a surface.<sup>25</sup> Furthermore, we have seen that assemblies in nonpolar solvents such as hexanes result in lower thicknesses and contact angles than those done in polar solvents such as methanol and THF. In this light, the removal of  $[\text{Au}(\text{CN})_2]^-$ ,  $[\text{Ag}(\text{CN})_2]^-$ , and  $[\text{Pt}(\text{CN})_4]^{2-}$  is a more plausible mechanism. However, attempts to acquire AFM images which show increased roughness of the gold surface for assemblies of **1** compared to **4** (due to the loss of  $[\text{Au}(\text{CN})_2]^-$ ) have so far been unsuccessful.

A brief discussion of the loss of the metal cyanide anion is warranted. First observation suggests this is problematic

(43) Friedrich, K. A.; Daum, W.; Klunker, C.; Knabben, D.; Stimming, U.; Ibach, H. *Surf. Sci.* **1995**, 335, 315–325.

(44) Hanks, T. W.; Ekland, R. A.; Emerson, K.; Larsen, R. D.; Jennings, P. W. *Organometallics* **1987**, 6, 28–32.

(45) Kishi, K.; Ikeda, S. *Surf. Sci.* **1981**, 107, 405–416.

(46) Kordis, J.; Gingerich, K. A.; Seyse, R. J. *J. Chem. Phys.* **1974**, 61, 5114–5121.

(47) Dietz, O.; Rayon, V. M.; Frenking, G. *Inorg. Chem.* **2003**, 42, 4977–4984.

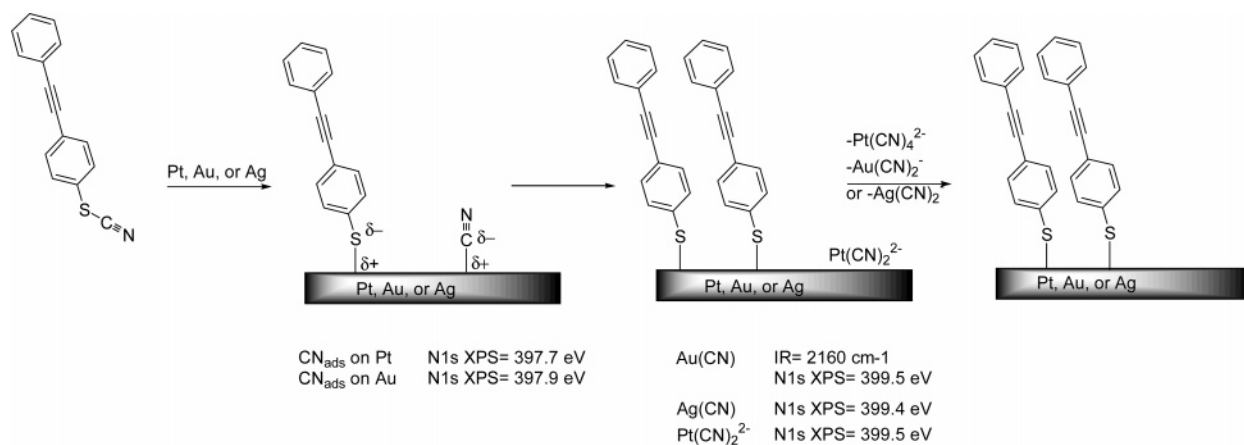


**Figure 11.** Refined mechanism for the assembly of thiocyanates onto metal surfaces based on XPS analysis of the surfaces.

as such salts are classically “insoluble” in organic solutions. However, the amount of charge dispersed in the solution is minimal, on the order of  $\sim 10^{-8}$  M. This is less than what is seen in the classical electrochemical cell without a salt bridge. The classical rules of “ionic species are insoluble in organic solutions” also fail as classical “insoluble” salts (i.e., AgCl,  $K_{\text{sp}} = 10^{-10}$  H<sub>2</sub>O) are soluble within the range that we claim. Also, even in freshly distilled organic solutions (as used for these assemblies), there are extraneous counterions available at these levels. Due to the extreme difficulty in directly observing this species, the nature or presence of a counterion will likely remain unknown.

Further justification for the cyanide leaching mechanism is required since it is accepted that platinum does not undergo etching by  $\text{CN}^-$  under standard conditions.<sup>20</sup> Yet we clearly see ratios of greater than 1:1 S to N on the surface (i.e., 4:1). Platinum is not etched by basic cyanide solutions due to the unfavorable oxidation of Pt to  $\text{Pt}^{2+}$  at no applied bias.<sup>48</sup> At applied positive voltages the reaction proceeds as seen in Figure 10. The oxidation of gold is more favorable and the reaction proceeds even at negative potentials. In our system the platinum must donate an electron for each cyanide adsorbed on the surface; thus, this problem is mitigated (Figure 11).

### Summary

In this paper we have demonstrated that the assembly mechanism for thiocyanates assembling on metal is similar for cases where the metal is platinum, silver, and gold. In these cases the S–CN bond is cleaved, leaving a species identical to that seen in free thiol assembly (Figure 11). In

most cases a small amount of nitrogen residue is often found on the surface. This nitrogen manifests itself as one of two species, the first of which is cyanide adsorbed on the metal surface (N 1s signal at 397.7 eV for Pt and 397.9 eV on Au). The second species (N 1s signal at 399.4–399.5 eV) is identical to intermediate species often seen during the etching of metal surface by cyanide:  $\text{Pt}(\text{CN})_2^{2-}$  and AuCN (Figure 11). For gold the residual nitrogen appears an average of one time on the surface for every four sulfurs bound to the surface. Contact angle measurements and ellipsometry suggest, in the case of the aliphatic species, that the adsorbed CN prevents complete coverage of thiolates on the surface. In the case of the aromatic species, the data suggest the adsorbed cyanide is partially incorporated in the monolayer and interferes with thiolate adsorption to a smaller degree. Last, comparison of results on evaporated gold and silver to those on TS gold allows us to suggest that surface morphology plays a major role in the expulsion of cyanide from the surface.

**Acknowledgment.** This work was supported by DARPA, via ONR and the AFOSR, and the NSF Penn State MRSEC. The NSF, CHEM 0075728, provided partial funds for the 400 MHz NMR. Trimethylsilylacetylene for compound preparation was donated by Dr. Ian Chester of FAR Laboratories and Dr. Radi Awartani of Petra Research, Inc. We thank Prof. David Allara, Prof. Jorge Seminario, Prof. Doug Natelson, and Drs. Bo Chen, Michael Stewart, Lam Yu, and Luis Agapito for their assistance.

**Supporting Information Available:** Synthetic details and characterization data are available online. This material is available free of charge via the Internet at <http://pubs.acs.org>.

(48) Dorin, R.; Woods, R. *J. Appl. Electrochem.* **1991**, *21*, 419–424.